

PAPER • OPEN ACCESS

The influence of polyethylene glycol on characteristic of Fe-N-TiO₂ photocatalyst and its activity for water splitting

To cite this article: S Priatmoko *et al* 2020 *J. Phys.: Conf. Ser.* **1567** 022022

View the [article online](#) for updates and enhancements.



IOP | ebooks™

Bringing together innovative digital publishing with leading authors from the global scientific community.

Start exploring the collection—download the first chapter of every title for free.

The influence of polyethylene glycol on characteristic of Fe-N-TiO₂ photocatalyst and its activity for water splitting

S Priatmoko*, R P Sadewo, Harjito and S K Rakainsa

Chemistry Department, Faculty of Mathematics and Natural Sciences, Universitas Negeri Semarang, Indonesia

*Corresponding author: sigitwarsono65@mail.unnes.ac.id

Abstract. Fe-N-TiO₂ photocatalyst has been used in water splitting to produce hydrogen. Templating agent and dopant modification intends to determine the optimum composition with the best characterization and the highest production rate in visible light. Fe-N-TiO₂ is synthesized using a sol-gel method with a various PEG and N weight percent. The variation of PEG is 2, 3, and 4% while N is 20, 25, and 30% w/w. Photocatalyst is characterized using DR-UV to find the band gap, XRD to see the crystallinity, and FTIR to know the functional group. Hydrogen gas from water splitting is analyzed using GC-TCD. Fe-N-TiO₂ with 20wt% N can decrease up band gap to 2.56 eV. Photocatalyst with 4% PEG accelerates gelation time to 164.33 hours. The calculation of PEG anatase phase is 86.86% while the crystallite size is 44.26 nm. Synthesized Fe-N-TiO₂ has major absorption at 520 cm⁻¹ which is a region of Ti-O. From the activity test, Fe-N-TiO₂ with 2% PEG and 20wt% N produces 0.076 μmol/hour hydrogen.

1. Introduction

Approximately 95% of hydrogen is obtained from fossil fuels while another 5% comes from water electrolysis [1]. As an alternative, photocatalytic water splitting is more promising method, since water is plentiful and renewable, also uses only sunlight and semiconductor photocatalyst [2]. Metal oxide semiconductor such as TiO₂, SrTiO₃, ZrO₂, Ta₂O₅, WO₃ and others are used as photocatalyst [3]. Usually, photocatalyst in water splitting are metal oxide that have wide band gap. TiO₂ is widely used because it is efficient, easy to make, non-toxic, inert, photostable and high oxidation ability [4]. However, all of that is limited by wide band gap, so it requires UV light to activate the photocatalyst. The efficiency of hydrogen production on TiO₂ is also low due to the relatively rapid recombination [5].

This deficiency need to be solved by modifying the TiO₂ photocatalyst. A lot of research has been made to inhibit recombination, one of them is by metal doping [6]. Cation-anion dopant in TiO₂ is able to decrease band gap and increase photocatalytic activity [7]. Fe is one of the metals that can inhibit recombination by capturing both charge carriers [3]. It is just that Fe can't decrease band gap as well as non-metallic dopants. New Study of TiO₂ absorption shifting to visible light is a non-metallic substitution of Oxygen side in TiO₂ lattice [8]. Non-metallic substitution show that N 2p hybridized with O 2p when the concentration exceed 4wt% [9]. However, N-TiO₂ can't inhibit recombination or increase photocatalytic activity as well as metal dopants. Template usage in TiO₂ synthesis by sol-gel method aims to control the morphology and particle structure [10]. The use of PEG as templating agent is due to nature of this compound which can be a structure-directing agent in photopolymerization reaction [11]. Beside all, currently there isn't known proper concentration of PEG usage for sol-gel method.



Based on that reason, a research is arranged which titled with synthesis of Fe-N-TiO₂ photocatalyst by sol-gel method for water splitting. This study will synthesized Fe-N-TiO₂ photocatalysts with the addition of various PEG and N.

2. Experimental Method

The tools used in this research are glass tool, analytical scale (AND HR-200), magnetic stirrer (Lab Line 1262-1), oven (Memmert Single DISPLAY U10), furnace (Thermolyne 79400), Xenon D1S lamp (35 W 4150 K), DR-UV Vis (DR 6000), XRD (Siemens D-5000), FTIR (Shimadzu Prastige-21), and GC-TCD (Shimatsu GC-2014).

The materials used in this research are titanium tetraisopropoxide (Aldrich, 97%), urea (Merck), iron(III) nitrate nonahydrate (Merck), nitric acid (Merck, 65%), absolute ethanol (Mallinckrodt, 99.99 %), polyethylene glycol (Merck, PEG 4000), and water.

The Fe-N-TiO₂ synthesis use sol-gel method with some modifications [12]. 10 mL of titanium tetraisopropoxide, iron(III) nonahydrate nitrate (0.5wt%), 5 mL of nitric acid, and 10 mL of water are dissolved in 200 mL of absolute ethanol. It is stirred for 30 minutes, resulting the solution A. PEG with variations of 2, 3, and 4% is dissolved in 30 mL of water in stirred state, resulting the solution B. Solution B is added slowly into solution A with stirring state until the solution becomes transparent, then it is stirred for 30 minutes. After the mixture became turbid, urea with variations of 20, 25, and 30wt% to TiO₂ is added and stirred for 2 hours. The mixture is aged for about 24 hours to form a fixed gel structure. The gel is dried at 100°C, then calcined at 500°C for 2 hours. Fe-N-TiO₂ with PEG 2% and N 20wt% is called TP2N20, PEG 2% and N 25wt% is called TP2N25, PEG 3% and N 20wt% is called TP3N20, and so on.

Fe-N-TiO₂ band gap is known from its absorbance to the wave. Measurement of absorbance is using DR-UV at room temperature with range 200-800 nm. Crystallinity is seen from peak pattern and intensity of the diffractogram. Intensity is seen with XRD using Cu K α radiation at 0.017° interval in the range 10°-80°. Transmittation spectra is obtained from FTIR with range 370-4000 cm⁻¹ and 2 cm⁻¹ resolution. Preparation is done at room temperature using KBr method.

Photocatalytic activity test is carried out in water splitting reaction with some modifications [13]. This test uses glass reactor with magnetic stirrer and Xenon D1S lamp. On the reactor side, there is a channel to the analysis instrument with a flowing gas system. At room temperature, 0.35 g of photocatalyst powder is added in reactor containing 500 mL of 30vol% water and glycerol mixture. Before the reaction, a test of reactor leak and purging is conducted by flowing 99.99% argon gas for 30 minutes at 100 cm³/min flow rate. The test reaction lasts for 2 hours with irradiation and stirring. The produced hydrogen is analyzed using GC-TCD.

3. Results and Discussion

In this study, the produced gel is a soft gel which aim for ease of gelation time observation. Based on the research, Soft Gel is formed slowly when pH is lower than in hard gel forming [14]. In Table 1, TP4N30 have the fastest gelation time with a decrease of 34.62%. PEG accretion makes gelation time faster where 4% PEG is the best addition. The hydrophilic oxygen atom in PEG molecule causes the colloid particles to be easily dispersed by hydrogen bonding with free hydroxyl groups on particle surface [15]. Urea usage as N precursor may also affect gelation time due to increased pH (pKa = 26.9).

The calculation result of DR-UV in Table 2 shows that more N additon then the band gap is getting bigger. 20wt% N can decrease band gap to 2.56 eV marked by absorption shift in TP2N20. This value is better than TP0N0 (3.15 eV) and other variations. Anatase have band gap above 3.2 eV, but the existence of rutile (3.02 eV) and brookite (2.96 eV) can affect TiO₂ band gap. Band gap determination uses Fochs method which is included in one of the Absorbtion edge methods [16].

Table 1. The gelation time of TiO₂ soft gel with PEG 4000 template.

Sample	PEG (%)	N (wt%)	Gelation time (hours)	Average (hours)
TP0N0	0	0	213.50	213.50
TP2N20	2	20	186.17	
TP2N25	2	25	211.50	195.03
TP2N30	2	30	187.42	
TP3N20	3	20	187.00	
TP3N25	3	25	163.75	179.25
TP3N30	3	30	187.00	
TP4N20	4	20	190.75	
TP4N25	4	25	162.67	164.33
TP4N30	4	30	139.58	

This method calculates the wavelength of the two-line intersections in absorbance spectra as shown in Figure 1. Co-dopant photocatalyst has more than one band gap due to the reflectance of each dopant so that Tauc plot with Kubelka-Munk function can't be used. In Fe-TiO₂, conduction band will shift towards lower energy due to the hybridization of Fe and Ti 3d orbital [1]. The shift also occurs in N-TiO₂ valence band heading to higher energy. The shift narrows Fe-N-TiO₂ energy gap so that electrons are easily excited.

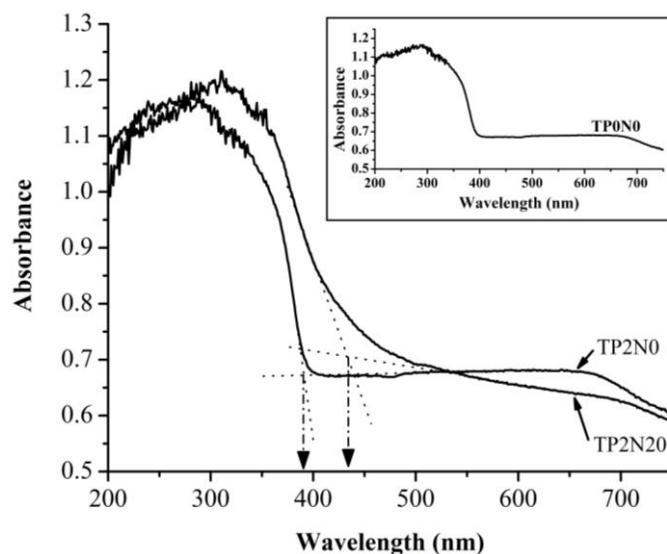


Figure 1. The wavelength intersection on TP0N0 (PEG 0% N 0wt%) (bottom) and TP2N20 (PEG 2%N 20wt%) (above).

Table 2. Band gap of Fe-N-TiO₂ photocatalyst sample.

Sample	PEG (%)	N (wt%)	Band gap (eV)
TP0N0	0	0	3.15
TP2N20	2	20	2.56
TP3N20	3	20	2.98
TP4N20	4	20	2.73
TP2N25	2	25	3.00
TP3N25	3	25	2.99
TP4N25	4	25	2.60
TP2N30	2	30	2.91
TP3N30	3	30	3.00
TP4N30	4	30	2.90

XRD diffractogram in Figure 2 shows 3 peak phases, it as anatase (25,43°), rutile (27,58°), and brookite (30,8°) which usually form at low pH and temperature. Soft gel synthesis with low pH conduce the brookite forming, but urea usage decrease the amount of brookite. Unformed Fe peak on diffractogram is caused by low Fe weight percent, small atomic size, and high dispersion on the surface [1]. Table 3 shows that TP2N20 provides better crystallinity than other variations with 86.86% anatase phase and 44.26 nm crystallite size. The increasement in N causes the anatase phase decrease, although the crystallite size becomes 48.66 nm due to increased size of crystallite grain growth. Reduction in anatase due to excessive addition of PEG and N is caused by the rearrangement of Ti & O distance due to N in the lattice structure [17]. This effect also applies to templating agent and causes irregular photopolymerization on condensation.

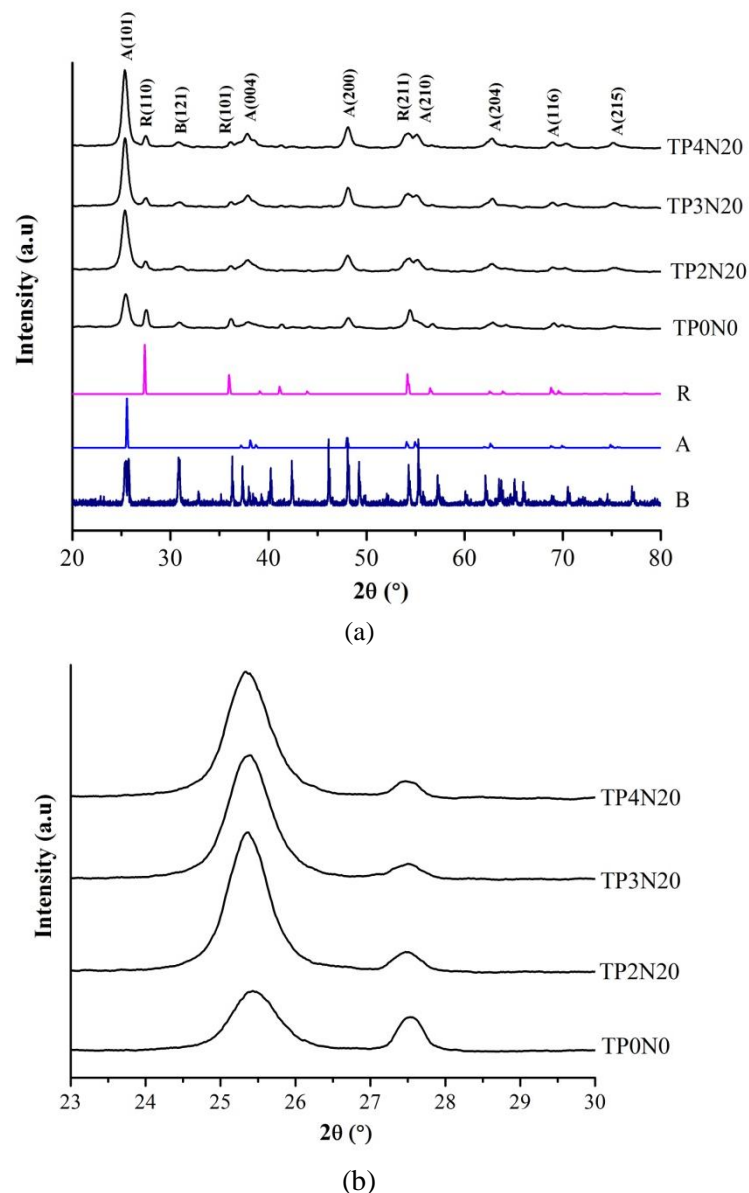


Figure 2. XRD Diffractogram with PEG variation (a) and enlargement in 2θ range of 20° - 35° (b). Notes: A = anatase, B = brookite, C = rutile.

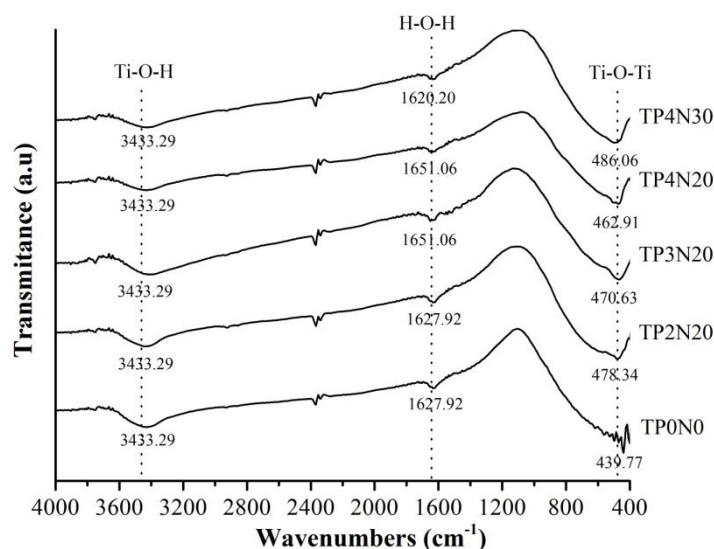
Table 3. Crystal phase and crystallite size of Fe-N-TiO₂ photocatalyst.

Sample	PEG (%)	N (wt%)	Crystal Phase (%)			Crystallite Size (nm)
			Anatase	Rutile	Brookite	
TP0N0	0	0	47.78	38.40	13.82	15.21
TP2N20	2	20	86.86	5.91	7.23	44.26
TP3N20	3	20	80.56	10.86	8.57	17.38
TP4N20	4	20	81.85	13.29	4.86	17.39
TP4N25	4	25	77.03	16.15	6.81	48.66

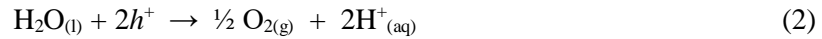
The transmittance spectra results in Figure 3 show the peak of the same spectral wave numbers in both samples, namely at wave numbers 520, 1635, and 3400 cm⁻¹. This matter means that the structure of TiO₂ bonds did not change after addition of N dopant and PEG templating agent. The wide peak at the wave number 520 cm⁻¹ corresponds to the symmetrical bonding of the stretching Ti-O-Ti functional group in the upper TiO₂ crystal [4]. The wave number 1635 cm⁻¹ shows bending O-H bonds of water molecules adsorbed on the photocatalyst surface of TiO₂, while the wave number 3400 cm⁻¹ is O-H stretching absorption of hydroxyl functional groups that bind to Ti atoms [18].

The hydroxyl function group shows that there are still Ti-OH bonds in the photocatalyst due to imperfect condensation reactions. This Ti-OH bond makes it easy for photocatalysts to bind water in the air through hydrogen bonds thereby reducing photocatalytic ability. However, in the Fe-N-TiO₂ photocatalyst, the intensity of the wave number of the hydroxyl group has decreased which shows a reduced Ti-OH bond. The addition of PEG as a templating agent can facilitate condensation reactions because this compound will form a ring-network structure when dissolved in water or ethanol and become a mold for the structure of TiO₂ [19].

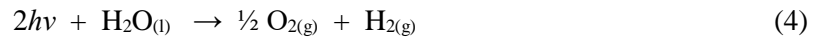
The peaks of organic functional group wave numbers such as C-H (2850 cm⁻¹ stretching, 1430 cm⁻¹ bending) or C-O (1073 cm⁻¹) are not seen in the transmittance spectra [20]. This proves that calcination with a temperature of 500°C can eliminate organic compounds during the synthesis process. Organic compounds such as PEG (Poly Ethylene Glycol) and ethanol can become impurities on TiO₂ photocatalysts if not removed. The existence of N is also not clearly seen because the peak wave numbers of 1060 and 1450 cm⁻¹ are not detected which describe the bond of Ti-N and Ti-O-N or nitrate groups [21]. With variations of the addition of 30% w/w, nitrogen cannot be substituted into the TiO₂ structure and only intercalated in the Ti-O-Ti bonding lattice or scattered on the photocatalyst surface.

Figure 3. Absorbance spectra of TP0N0 (TiO₂) and TP4N30 (Fe-N-TiO₂).

In the process of decomposition of water, photocatalysts need photon energy from light sources of a certain wavelength to produce electrons in the conduction band and holes in the valence band. The hole will split water molecules into oxygen gas and hydrogen ions and electrons reduce hydrogen ions to hydrogen gas as follows.



Overall, the above equation is simplified to [22],

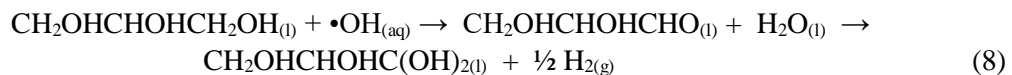


In this study, the water decomposition process uses a 30% glycerol solution (a mixture of water and glycerol) which has 2 main functions. Besides being as a sacrificial agent that prevents recombination of holes and electron, glycerol also serves to increase the amount of hydrogen production by oxidizing and producing several intermediate compounds followed by the final hydrogen product.

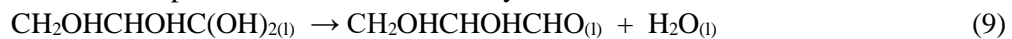
Hydrogen production from a mixture of water and glycerol consists of two mechanisms, namely photo-splitting of water and photo-reforming of glycerol (glycerol reform) [23]. Water will decompose according to the water splitting reaction and the hydroxyl free radicals produced will be more likely to react with glycerol than to form O₂ gas.



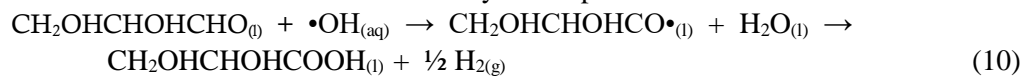
Hydroxyl free radicals will enter the glycerol reform mechanism and produce the final product of hydrogen.



An unstable intermediate compound will become an aldehyde.



Hydroxyl free radicals will continue to oxidize the aldehyde compounds formed.



The carboxyl group will be oxidized by holes and decarboxylate.



The alcohol compound will again be oxidized by hydroxyl free radicals and produce a carboxyl group. The reaction will continue to repeat and stop when the final results obtained in the form of CO₂ and H₂O gas.

The results of the calculation of the rate of hydrogen production from the Gas Chromatograph-Thermal Conductivity Detector (GC-TCD) data in Figure 4.8 show that TP2N20 produces more hydrogen gas than TP4N25. Both of these samples have large crystallite sizes thus providing increased catalytic ability, but the low crystallinity of TP4N25 causes the production of hydrogen gas to be less than TP2N20 [24].

In the first 30 minutes, it is clear that the Fe-N-TiO₂ photocatalyst can already produce hydrogen gas. With a low band gap value (2.5-2.6 eV), photocatalysts can be excited during purging

even without irradiating Xenon DIS lamps. However, the production of hydrogen gas from the test reaction was only 0.076 $\mu\text{mol}/\text{hour}$ at TP2N20 and 0.02 $\mu\text{mol} / \text{hour}$ at TP4N25. This amount is very small when compared to UV light irradiation which can produce hydrogen gas of 2.98 $\mu\text{mol} / \text{hour}$ [25]. In TP0N0, no hydrogen gas was found due to a high band gap (3.15 eV) so that there was no excitation with Xenon lighting.

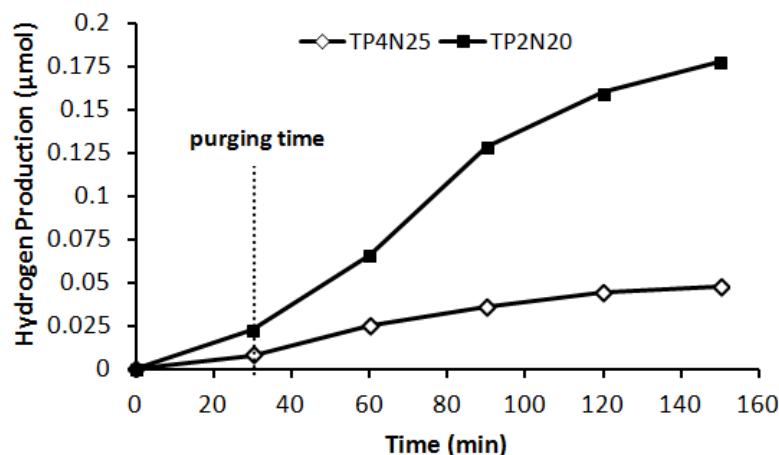


Figure 4. The hydrogen production rate of Fe-N-TiO₂ photocatalyst.

4. Conclusion

The optimum addition of N dopant is 20wt% with band gap reach 2.56 eV and greater as the dopant increasement marked by the absorption shift. 4% PEG reduces gelation time to 34.62% but excessive usage cause reduced anatase phase and crystallite size. The best crystallinity is shown by 2% PEG with 86.86% anatase phase and 44.26 nm crystallite size. With small band gap and high crystallinity, TP2N20 can excite in visible light and produce 0.076 $\mu\text{mol}/\text{hr}$ hydrogen.

5. Acknowledgment

The authors gratefully acknowledge the support of the Chemistry Laboratory, Faculty of Mathematics and Natural Sciences, Semarang State University, Laboratory of Sustainable Energy, Faculty of Engineering, University of Indonesia and Indonesian Institute of Sciences.

References

- [1] Reddy J K, Lalitha K, Reddy P V L, Sadanandam G, Subrahmanyam M, and Kumari V D, 2014, *Catalysis Letters*, **144**(2): 340–346.
- [2] Leung D Y C, Fu X, Wang C, Ni M, Leung M K H, Wang X, and Fu X, 2010, *ChemSusChem*, **3**(6): 681–694.
- [3] Dholam R, Patel N, Adami M, and Miotello A, 2009, *International Association for Hydrogen Energy*, **34**(13): 5337–5346.
- [4] Ubonchonlakatea K, Sikong L, and Saito F, 2012, *Procedia Engineering*, **32**:656–662.
- [5] Xu S, Du A J, Liu J, Ng J, and Sun D D, 2011, *International Journal of Hydrogen Energy*, **36**(11): 6560–6568.
- [6] Choi W, Termin A, and Hoffmann M R, 1994, *The Journal of Physical Chemistry*, **98**(51): 13669–13679.
- [6] Sasikala R, Shirole A R, Sudarsan V, Sudakar C, Naik R, Rao R, and Bharadwaj S R, 2010 *Applied Catalysis A: General*, **377**(1): 47–54.
- [7] Asahi R, Morikawa T, Ohwaki T, Aoki K, and Taga Y, 2001, *Science*, **293**(5528): 269–271.
- [8] Kuvarega A T, Krause R W M, and Mamba B B 2011 *The Journal of Physical Chemistry C*, **115**(45): 22110–22120.

- [9] Schubert U and Hüsing N, 2012, *Synthesis of Inorganic Materials* (Weinheim: Wiley-VCH Verlag GmbH)
- [10] Jiao J, Xu Q, Li L, Tsubasa T, and Kobayashi T, 2008, *Colloid and Polymer Science*, **286**(13): 1485-1491.
- [11] Zhang K, Wang X, Guo X, He T, and Feng Y, 2014, *Journal of Nanoparticle Research*, **16**(2): 1-9.
- [12] Priatmoko S, Cahyono E, Wahyuni S, Kusumastuti E, and Prambasto SBU, 2014, *9th Joint Conference on Chemistry*. Semarang: Unnes Press.
- [13] Chong M N, Tneu Z Y, Poh P E, Jin B, and Aryal R 2015 *Journal of the Taiwan Institute of Chemical Engineers*, **50**: 288-296.
- [14] Han M Y, Ou Y, Chen W, and Deng L 2009 *Journal of Alloys and Compound*, **474**(1): 185-189.
- [15] Prasetyoko D, Fansuri H, Ni'mah Y L, and Fadlan A, 2016, *Karakterisasi Struktur Padatan* (Yogyakarta: Deepublish).
- [16] Purnama A, Priatmoko S, and Wahyuni S, 2013, *Indonesian Journal of Chemical Science*. **2**(3): 1-7.
- [17] Khodadadi B, Sabeti B M, Moradi S, Azar A, and Farshid SR, 2012, *Journal of Applied Chemical Research*, **20**(1): 36-44.
- [18] Huang X, Meng L, Du M, and Li Y, 2016, *Journal of Materials Science: Materials in Electronics*, **27**: 7222–7226
- [19] Wang, H., Peng, R., Hood, Z.D., Naguib, M., Adhikari, S.P., Wu,Z., 2016. *Chem. Sus. Chem.* **9**: 1490–1497
- [20] Pang YL, and Abdullah AZ, 2013, *CLEAN - Soil Air Water*, **41**(8)
- [21] Lin L, Wang H, Jiang W, Mkaouar AR, Xu P, 2017, *Journal of Hazardous Materials*, **333**: 162-168.
- [22] Slamet D, Tristantini D, Valentina, and Ibadurrohman M, 2013, *International Journal of Energy Research*, **37**(11): 1372-1381.
- [23] Luisetto I, Tuti S, Battocchio C, Mastro S L, and Sodo A, 2015, *Applied Catalysis A: General*, **500**: 12-22.
- [24] Liu S-H, and Syu H-R, 2012, *Applied Energy*, **100**: 148–154